A COLLECTION OF BENCHMARK IMAGES FOR TRAFFIC SIGN RESEARCH

Xiaohong W. Gao
School of Engineering and Information Sciences, Middlesex University, London, NW4 4BT, United Kingdom,
x.gao@mdx.ac.uk

ABSTRACT

This paper details a collection of traffic signs that has been made available online to meet the current need of lack of standard datasets for evaluation and comparison of existing and future developed recognition systems of traffic signs, leading to the exploration of the breath of innovations and applications in the field. Examples on how to apply these data are also described with comparisons between a number of approaches on segmentations. This collection aims at improving the accuracy of sign recognition systems and expediting the processing speed. Within this remit, the images in the collection opt for 2D still pictures and are taken under controlled viewing conditions on London roads at the UK. The standard sign database employs British road signs (143 images), which are available at http://www.mitime.org/traffic_signs/, together with the collection (128 images) in this study.

Key words— traffic signs, segmentation, recognition, benchmark datasets, CIECAM

1. INTRODUCTION

Recognition of traffic signs has lent itself well to a long-standing research topic that continuously attracts wider interests, partly because of its potential application to intelligent systems for supporting drivers and unmanned vehicles, and partly due to the fact that the challenges to develop such a system still remain. Usually, with an automatic system of sign recognition, video images along a road are captured using one or more cameras mounted upon a moving vehicle. While at the same time, the task of image processing takes place on a frame-by-frame basis to detect and recognise signs. If a sign is identified, the system will provides with drivers a matching one obtained from a standard database that has been stored in the system in advance. The key challenges here are the processing speed to be in real-time and the accuracy of recognition to be precise. For example, if the speed of a video recording arrives at 8 frames or 32 frames per second, the processing speed should arrive at 0.125 or 0.031 second per frame. To this end, most developed systems take two steps to process one frame, which are, broadly speaking, segmentation or detection and recognition [1, 2]. Since majority of the contents (~90%) of a recorded picture of a road scene are not signs, the step of segmentation can help the system to focus on those remaining 10% regions to speed up the process. In addition to study spatial information on each frame, temporal information in-between frames can be exploited by tracking the same sign appearing on successive frames [3-5], intending to save the time of re-processing of the same sign. However, tracking itself sometimes tends to be time-consuming especially when there is a new sign appearing on the same frame or the original sign is occluded partially.

On the other hand, the stages of detection and recognition can be treated either in a collective way or separated way. For example, at [6], FFT (Fast Fourier Transform) has been applied in the detection stage, resulting in the act of recognition straight forward. Whereas at [1, 2], self-organising map and SVMs (Support Vectors Machines) have been developed for these tasks to be treated as a whole. To compensate the change of illuminations and partial occlusions, a multi-class classification method with β-correction decoding strategy has been developed at [7].

At present, the approaches developed for processing a single image are towards taking advantages of the characteristics contained within signs, mainly colour and shape as demonstrated in Fig.1 where a number of standard signs are given [8, 9]. Based on the information of colour and shape, vision model-based [10, 11] and neural network based approaches [3] have been developed to segment and subsequently recognise signs. As a result, while the research work of state of the art has been focusing on processing video images, much of the progress still draws on the investigation of approaches of sign recognition obtained from a single frame based on spatial information, pointing to the value of the establishment of a collection of benchmark images.

Sign Examples	Meaning	Colour	Geometric Shape
	Turn left ahead	Blue	Circle
	One-way traffic	Blue	Rectangle
	No entry for vehicular traffic	Red	Circle
	Stop and give way	Red	Octagon
	Give way	Red	Triangle

Fig. 1. Examples of signs on British roads.

Significantly, as also stressed at [6], the lack of benchmark sign databases has made it difficult to compare the existing methods and to evaluate the effects on those approaches when the change of viewing conditions occurs, one of the major factors that alter the accuracy of a system. To cement this gap, many current research has been working on off-line video clips [12] to evaluate training sets in an effort to cover a wider range of viewing conditions, which has inspired the release of the collection of

images in this study and that are available on line at http://www.mitime.org/traffic_signs/, together with the methods to employ them as a training dataset should viewing conditions are to be taken into account. These pictures are in a form of 2D still images concerning with spatial information and are taken under controlled viewing conditions on London roads at the UK in order to account for the requirement of variety approaches for sign detection and recognition. In addition, the release of this collection is also to meet the requirement by numerous researchers searching for training datasets. It is hence in our intention to establish a benchmark collection of sign images for the research community, making a step forward towards the development of a robust system of traffic sign recognition.

2. DATA COLLECTION

This collection serves to show the change of weather conditions and focuses on sunny, cloudy and rainy days since understandably most methods work better on sunny days than on the others. Fig. 2 demonstrates a typical example of the collection showing a similar scene but are captured under different weather conditions, i.e., under sunny and rainy days respectively. Whereas Fig. 3 shows the degree of a sign can be distorted in a captured image.

The collection includes one hundred and twenty-eight images consisted of 48, 27, and 53 pictures taken under sunny, cloudy and rainy days respectively. The resolution of an image is 640x480 pixels with a format in TIFF. Standard signs of 143 from British high ways are also included in the collection, which will be in need during recognition stage. To ensure a picture that is taken visually match the viewing conditions, several measures are considered to get correct settings of camera parameters.

Fig.2. Examples of the change of colour appearance under different weather conditions, i.e, sunny (top) and rainy (bottom) days.

Shadow	Rotation	NOISE	Same shape (circle) different meanings

Fig. 3. Distorted signs in the captured images.

2.1. Camera colour calibration

Olympus Digital Camera C-3030 has been used throughout the collection, one of the best at the time with the characteristics of high resolution (3.34-mega pixel Charged Couple Device (CCD)) and a flexible facility of manual control including shutter, aperture or manual exposure modes. For shooting each picture, the white balance is set first, by the assistance of a white paper or the white region of a sign as shown in Fig. 4 to calibrate the camera. It has been found out that there is no significant difference when either of them is employed. For example, the mean value of 15 measurements of chromaticity values from white signs is (0.3143, 0.316) and is (0.313, 0.311) from a white board under different surroundings. These values apply to all weather conditions, i.e., under sunny, cloudy or rainy days. The correlated colour temperature during the shooting ranged from 5000K to 7000K with an average of 6500K (D65) during day time, while luminance levels varying from 5 to 2500 candela square meters (cd/m^2).

Fig.4. Reference white measurement from white board (left) and white colour of traffic signs at the same view condition (right).

The image format is in TIFF, the format that is used to transfer into a monitor that has been calibrated in advance using Pantone ColorVision Spyder under a setting of D65. Physical measurement for each sign, i.e., red, or blue colours, in each scene has also taken place using a Chroma Meter Minolta CS-100A to get physical colour information of x, y, and Y values in terms of CIE (Commission internationale de l'éclairage) [13] tristimulus colour space. When these images are downloaded to a computer, they are represented using RGB (red, green and blue) space. For example, a red colour can be represented as 0.63, 0.35 and 23 in terms of x, y, and Y respectively and in a RGB space as 250, 5, and 5 in a computer with a resolution of 8-bit, yielding R (or G, or B) value ranging from 0 to 2^8-1 (=255).

2.2. Establishment of a transformation matrix from RGB to XYZ

In order to find the manual setting parameters of a camera, such as aperture, exposure time, and speed, a transformation matrix (a camera model) from a camera to a monitor is established using the following procedures as shown in Fig. 5. Firstly, a Macbeth

ColourChecker is placed under a standard viewing condition, say D65 with Y=100, i.e., a normalised luminance level for a reference white under a viewing cabinet. Then the captured picture of the checker is transferred to a monitor calibrated under the same viewing condition, i.e., D65 and Y=100. After the measurement of x, y, and Y values using CS-100A on each of 24 colours on the checker both under viewing cabinet and on a computer screen, a matrix can then be obtained as given in Eq. (1) using least squares regression method, which can be applied as a camera model. Non-linear models, such as polynomial, can also be applied depending on the cameras.

$$\begin{bmatrix} X \\ Y \\ Z \end{bmatrix} = \begin{bmatrix} 0.2169 & 0.1068 & 0.048 \\ 0.1671 & 0.2068 & 0.0183 \\ 0.1319 & -0.0249 & 0.3209 \end{bmatrix} \cdot \begin{bmatrix} R \\ G \\ B \end{bmatrix} \quad (1)$$

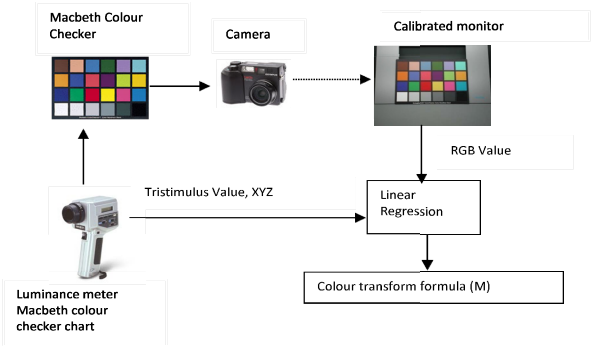

Fig. 5. Method of establishment of a colour transformation matrix from RGB to XYZ.

2.3. Setting of camera parameters

Since most cameras have a facility of automated compensation to make a darker lighting condition appear lighter, far beyond a real viewing condition, in this study, manual setting are practiced. Under each weather condition, the camera settings, including aperture, exposure time, and speed, are obtained using the following procedures. At each combination of camera settings (for each viewing condition, each setting is within a certain range), a captured picture e.g., a Macbeth Checker, is transferred to a calibrated monitor. The measurement of x, and y values of them then take place between the checker and its image on a monitor. After transformation using Eq. (1), the two triple values of x, y, and Y should be similar to each other, whereas Y value has been normalised to 100 for reference white as explained in Fig. 4. The triple values bearing the smallest CIELAB ΔE value will be considered the best setting of the camera at the intended viewing environment. This process however takes only once for each of the three viewing conditions, i.e., on sunny, cloudy or rainy days.

3. DATA ANALYSIS

Experiment has been conducted to see whether the change of luminance levels (e.g., in the early morning or at noon) effects the appearance of a sign. To do this, each red or blue sign has been measured using a chroma meter CS-100A over a period of 12 hours during daytime with varying luminance levels ranging from 5 to 2500 cd/m^2. With the measurement represented in x, y, and Y values, they are then converted into Chroma and Hue values, the more subjective terms than x, y and Y, using a colour appearance model CIECAM97s [14, 15]. It can be found that after the calculation from the model, the values of hue and chroma scarcely change. The standard deviations for red hue and red chroma are 0.62 and 1.10 respectively, giving rise to less than 1% variations. Therefore, it is assumed that the visual colours in terms of hue and chroma are illuminance invariant, which can lead to a reliable segmentation of signs based only on hue and chroma values, being consistent with the theory of luminance adaptation of the human vision [16].

3.1. Application of the data collection for sign detection and segmentation

To start processing a frame of video images, detection and segmentation of potential signs usually take place first in order to pay more attention to the potential regions of signs that occupies around only 10% of a scene, speeding up the process of sign recognition. As such, much work employs colour-based approach for colour signals one of the major characters of signs.

For the application of colour appearance models, e.g., CIECAM97s or CIECAM02, a later version, parameters of viewing environment, such as reference white, background and luminance levels (e.g., average, dim, and dark) are required first, which fortunately can be found out through images themselves. For instance, the 'whitest' region in an image, i.e., a pixel carries the highest and similar R, G, B values, such as R=250, G=245, and B=251, can be treated as a reference white due to the ability of chromatic adaptation of human vision systems. Although this collection has been classified into three groups manually, this classification can also be performed automatically based on the appearance of a sky and a road on images using a thresholding approach. Then based on Eq. (1), an image in a RGB space can be converted into XYZ space, allowing a colour appearance model to predict colour attributes in terms of hue and chroma using Eq. (2). The range of known signs for each attribute can then be found out that subsequently is applied to threshold an input image to segment potential signs. In the case of CIECAM97s, it takes into account the tristimulus values (X, Y, and Z) of a stimulus, its background, its surround, the adapting stimulus, the luminance level, and other factors such as cognitive discounting of the illuminant. The output of the colour appearance model includes mathematical correlates for perceptual attributes that are brightness, lightness, colourfulness, chroma, saturation, and hue, which are calculated in the following formulas. For this collection of data, the surrounding viewing parameters are set to an 'average' with c=0.69, F=1.0, and Nc=1, with the background luminance being Yb=20.

$$J = 100\left(\frac{A}{A_w}\right)^{cz}$$

$$\mathrm{C} = 2.44\mathrm{S}^{0.69}\left(\frac{\mathrm{J}}{100}\right)^{0.67\mathrm{N}}(1.64 - 0.29^{\mathrm{N}}) \quad (2)$$

$$\mathrm{h} = \tan^{-1}\left(\frac{\mathrm{b}}{\mathrm{a}}\right)$$

where

$$\mathrm{A} = \left[2\mathrm{R}'_{\mathrm{A}} + \mathrm{G}'_{\mathrm{A}} + \left(\frac{1}{20}\right)\mathrm{B}'_{\mathrm{A}} - 3.05\right]\mathrm{N}_{\mathrm{BB}}$$

$$\mathbf{s} = \frac{\mathbf{50(a^2+b^2)^{\frac{1}{2}}100e\left(\frac{10}{13}\right)N_cN_{cb}}}{\mathbf{R'_a+G'_a+\left(\frac{21}{20}\right)B'_a}} \quad (3)$$

$$a = R'_a - \frac{12G'_a}{11} + \frac{B'_a}{11}$$

$$\mathrm{B} = \left(\frac{1}{9}\right)(\mathrm{R'_A} + \mathrm{G'_A} - 2\mathrm{B'_A})$$

and R'_a, G'_a, B'_a are the post adaptation cone responses and A_W is the A value for reference white. Constants N_{bb}, N_{cb} are calculated as

$$N_{bb} = N_{cb} = 0.725(\frac{1}{n})^{0.2} \quad (4)$$

where $n = \frac{Y_b}{Y_W}$, and $\mathrm{Y_b}$ and $\mathrm{Y_w}$ the Y values for the stimulus and reference white, respectively, in addition to $z = 1 + Fn^{1/2}$.

TABLE I
THE RANGE OF HUE AND CHROMA CALCULATED USING CIECAM97S UNDER DIFFERENT WEATHER CONDITIONS

Weather conditions	Hue		Chroma	
	Red	Blue	Red	Blue
Sunny	375-411	287-305	31-43	37-59
Cloudy	370-413	275-290	25-45	30-65
Rainy	345-405	280-305	30-50	35-60

TABLE I lists the range of thresholds for this group of images using CIECAM97s. For many other colour spaces, for instance HSI (Hue, Saturation and Intensity), the weather conditions may not be as crucial, the application of the collection can simply be processed to convert RGB values from an image into HSI space and to find a group of thresholding ranges of colour attributes in terms of hue, saturation and intensity, to be explained below at Section 4.

3.2 Application of a standard dataset for sign recognition

To recognise a sign, a standard database usually has to be in place in order to show drivers a high quality sign that has been recognised as well as to identify a potential sign being one of those in the database. For example, in Fig. 6, a collection of British road signs are given as a standard dataset, whereas Fig. 7 depicts an interface of the recognition system. In Fig. 7, although five regions have been segmented as potential signs (left bottom with green boxes), only three of them are recognized as signs and marked with green boxes on the original image at top left. The diagram at right bottom shows the recognition rate and the standard signs if a segment is recognized. Otherwise, a blank will be given on the right, corresponding to the left segment, which can also be demonstrated as the number in the 'Result' box. It indicates the feature distance between a segmented sign and the matched one, which is the biggest (30) in comparison with the rest of signs. Non-recognised signs will carry a distance smaller than a threshold, which in our case is 25 that is found out empirically and to be discussed below.

Since a segmented image has much smaller size, e.g., being a normalised size of 40 x 40 pixels, elaborated algorithms can be employed at this stage without affecting the overall processing time substantially. The procedure can be either based on the information of shapes of a sign or the other approaches. In this study, an extension of Behaviour Model of Vision (BMV) [17] has been applied to compare segmented images with a standard database and has the characteristics of invariant to scale, rotation, noise, shift and in part point of view. The basic structure and operations in the BMV consist of:

(i) an image in each sensor fixation point is described by oriented segments extracted in the vicinity of each of 49 sensor nodes;

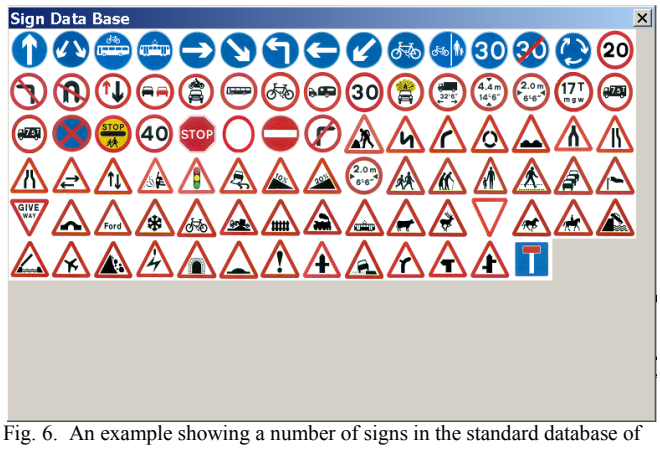

Fig. 6. An example showing a number of signs in the standard database of British Road Signs.

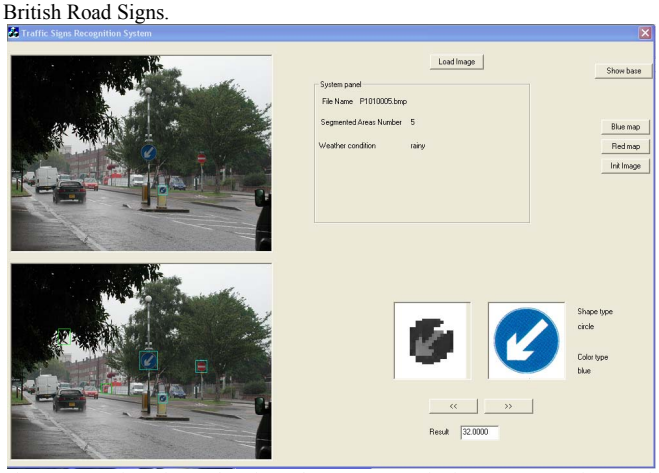

Fig. 7. An interface showing the process of sign segmentation and recognition.

(ii) the sensor nodes are located at the intersections of sixteen radiating lines and three concentric circles, each with a different length of radius;

(iii) orientation of segments in the vicinity of each sensor node is determined by means of the calculation of the differences between two oriented Gaussian functions with spatially shifted centres having the step of 22.5°;

(iv) space-variant representation of image features is emulated by Gaussian convolution with different kernels increasing with the distance from the sensor centre.

The 49-dimension vector for a potential sign is then compared with a feature database of images in the standard database, in our case the British Road Signs (BRS), that has been calculated in advance, by using Eq.(5):

$$K^b = \sum_{i=0}^{i\leq 49}\left[sgn\left(Or_i^b - Or_i^{rw}\right)\cdot\left(1 - abs\left(\rho_i^b - \rho_i^{rw}\right)\right)\right] \quad (5)$$

$$sgn(x) = \begin{cases} 1, if\ x = 0 \\ 0, otherwise \end{cases}$$

where $\mathrm{Or_i}$ is dominating orientation extracted from the context area of a given IW (input window) node (orientations are determined by

the step 22.5° and indicated as 1, 2, 3…., 16), whereas superscript b stands for images from a database (i.e., BRS) and rw the real world image segmented using colour-based approach. In addition, ρ is the density of a dominating oriented segment in the vicinity of the given IW node. Preliminary results have shown that minimal value of resulting K^b is 25. Otherwise the region of interest will be considered a false sign and is rejected. As given in Fig. 7, the segmented region of the top green box with tree leaves in it shown at the bottom-left of Fig. 7, has been rejected during the phase of recognition even though it has been segmented as a potential sign. The recognition rate using the BMV model after segmentation is listed in TABLE II and demonstrated in Fig. 8.

TABLE II
RECOGNITION RATE UNDER THREE WEATHER CONDITIONS

Weather	Potential signs after segmentation	Correct recognition	Recognition rate
Sunny	50	48	96%
Cloudy	29	27	94%
Rainy	48	44	93%

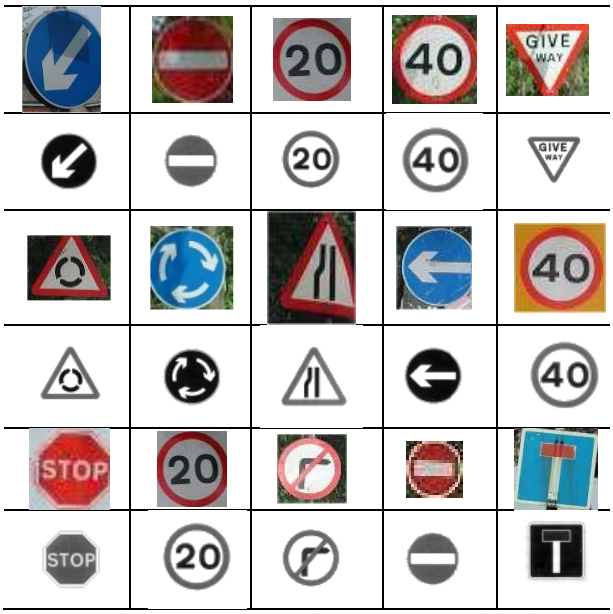

Fig. 8. Examples of recognition results using BMV model, where rows 1, 3, and 4 are the segments and rows 2, 4, and 6 (in grey-level) are the corresponding recognized signs for the upper rows respectively.

4. COMPARISON OF SEGMENTATIONs WITH THE OTHER COLOUR SPACES

Based on the dataset of this collection, comparison on the performance of segmentation with the other colour-based approaches is carried out. Two measures of accuracy are employed to compare the results including *probability of correct detection* (P_c), and *probability of false detection* (P_f), which are calculated using Eqs. (6) and (7) respectively.

$$P_c = \frac{number\ of\ segmented\ regions\ with\ signs}{number\ of\ total\ signs} \times 100\% \qquad (6)$$

$$P_f = \frac{number\ of\ segmented\ regions\ with\ no\ signs}{total\ number\ of\ segmented\ regions} \times 100\% \qquad (7)$$

Hence, for each approach, a higher P_c and lower P_f indicate its better performance on segmentation.

Four colour spaces/models that have been widely applied on colour segmentations are compared, including HIS, CIELUV, RGB, and CIECAM97s. Once again, 128 pictures in the collection are applied that contain 142 visible traffic signs. It should be noted that the training dataset that are used to obtain thresholds for each method are different from this collection of 128 images. For HSI [18] space, hue (H), saturation (S) and intensity (I) are calculated using the formula of Eq. (8).

$$H = cos^{-1}\left\{\frac{(R-G)+(R-B)}{2\sqrt{(R-G)^2+(R-B)(G-B)}}\right\}$$
$$R \neq G\ or\ R \neq B$$
$$S = Max(R,G,B) - Min(R,G,B) \qquad (8)$$
$$I = \frac{R+G+B}{3}$$

Whereas for CIELUV, H (hue), C (chorma) and L(lightness) are calculated in Eq. (9) [16].

$$L^* = 116(\tfrac{Y}{Y_0})^{1/3} - 16 \quad \text{if } Y/Y_0 > 0.008856$$
$$L^* = 903.3(\tfrac{Y}{Y_0}) \quad \text{if } Y/Y_0 <= 0.008856$$
$$u^* = 13L*(u' - u'_0)$$
$$v^* = 13L*(v' - v'_0) \qquad (9)$$
$$H = \tan^{-1}(v^*/u^*)$$
$$C = \sqrt{(u^*)^2 + (v^*)^2}$$

where y_0, u_0, v_0, are the y, u, v values for a reference white that can be obtained from the 'whitest region' in an image as discussed at section 2.1.

In addition, comparison with RGB space is performed on a calibrated monitor. The calibration setting is the average daylight of D65 for all weather conditions. Based on the preliminary evaluation of RGB composition for traffic signs using a training dataset, the ranges of [35, 255], [-20, 20], [15, 230], [5, 85] are determined for signs R-B, G-R, G-R, and B-G respectively. Moreover, while determining each segmented region as a potential traffic sign, two additional conditions should be taken into consideration. One is the size of clustered colour blobs that should be no less than 10x10 pixels. The other is that the ratio of width/height of a segmented region should be in a range of 0.5-1.5. In this way, the amount of segmented regions can be reduced as demonstrated in Table III where the number of regions that are falsely segmented reaches up to 288 under the sunny lighting condition. Table III also gives the comparison results of the aforementioned 4 methods on segmentation.

TABLE III
SEGMENTATION RESULTS BY FOUR COLOUR SPACES: CIECAM97, HSI, CIELUV, AND RGB

Weather condition	Total signs	Colour space	Results			
			Correct Seg.	False Seg.	*Pc (%)*	*Pf (%)*
sunny	53	*HCJ* (CAM 97s)	50	15	**94**	23
		HSI	46	19	88	29
		HCL (LUV)	46	17	88	27
		RGB	47	**288**	88	**86**

cloudy	32	*HCJ* (CAM 97s)	29	11	**90**	28
		HSI	24	14	77	37
		HCL (LUV)	26	12	82	32
		RGB	26	55	83	**68**
rainy	57	*HCJ* (CAM 97s)	48	18	**85**	27
		HSI	41	26	73	39
		HCL (LUV)	43	24	76	36
		RGB	47	87	82%	**65**

From TABLE III, it can be seen that CIECAM97s out performs the others on segmentation with up to 94% accuracy rate for sunny days in comparison with 88% for the others. Although the approach based on RGB-space gives higher correct detection rates (as shown in **Bold** numbers) than those based on HSI and CIELUV, it gives the worst false positive detection under all three weather conditions (i.e, 88%, 68% and 65% respectively), which, to some extent, can be circumvented by increasing the clustering size while grouping those segmented pixels to form a region.

5. CONCLUSION AND DISCUSSION

This paper details a collection of a dataset of traffic signs in 2D still images. It is anticipated that this collection serves as a benchmark dataset that can be utilised both to evaluate existing approaches and to develop future accurate recognition methods for traffic signs, arriving at an intelligent, robust driver assistant system. The focus here is on the improvement of accuracy of the methods on segmentation and recognition, whereas processing speed is another challenge to be faced to in order to equip these systems in real-time. At present, the processing time for segmentation using CIECAM97s is 1.8 seconds due to its complexity of calculations. However, as little as 0.19 second has been achieved at recognition stage using BMV, leading to 2 seconds for processing one frame of image. When processing video images, there are normally eight frames in 1 second, suggesting the total time (= segmentation time + recognition time) should be at 0.25 seconds per frame. Therefore, more work needs to be done to further optimise the algorithms for segmentation and recognition in order to meet the demand of real time processing. Although the correct segmentation rate is less than 100% while applying CIECAM97s, the main reason is the size of signs in an image being too small in some scenes, which can be overcome while processing video images for the same signs of interest will gradually appear larger when driving closer. Consequently the future work will be focus on collections of video images under controlled viewing conditions in order to fulfill the requirements by different methodologies.

6. ACKNOWLEDGMENT

This project was in part funded by The Royal Society at the UK. Their support is gratefully acknowledged. The author would also like to thank Dr. Kunbin Hong, who took all the pictures collected in the database as part of his PhD study.

7. REFERENCES

[1] M. S. Prieto, A.R. Allen, Using self-organising maps in the detection and recognition of road signs, *Image and Vision Computing*, 27:673–683, 2009.

[2] S. M. Bascon, J. A. Rodriguez, S. L. Arroyo, A. F. Caballero, An optimization on pictogram identification for the road-sign recognition task using SVMs, *Computer Vision and Image Understan*ding 114:373-383, 2010.

[3] C.Y. Fang, S.W. Chen, and Chiou-Shann Fuh, Road-Sign Detection and Tracking, *IEEE Transactions on Vehicular Technology*, 52 (5): 1329-1341, 2003.

[4] P. G. Jimenez, S. M. Bascon, A. L. Arroyo, F. L., Ferreras, Traffic sign shape classification and localization based on the normalized FFT of the signature of blobs and 2D homographies, *Signal Processing*, 88(12):2943-2955. 2008.

[5] A. Ruta, Y. Li, X. Liu, Real-time traffic sign recognition from video by class-specific discriminative features, *Pattern Recognition*, 43(1): 416-430, 2010.

[6] S. Miyata, A. Yanou, H. Nakamura, S. Takehara, Road sign feature extraction and recognition using dynamic image processing, *International Journal of Innovative Computing, Information and Control*, 5(11):4105-4113, 2009.

[7] S. Escalera, O. Pujol, P. Radeva, Traffic sign recognition system with β –correction, *Machine Vision and Application,* 21 (2):99-111, 2010.

[8] P. Paclík, J. Novovicová, P. Pudil, and P. Somol, *Road* Sign Classification using the Laplace Kernel Classifier*, Pattern Recognition Letters*, 21(13-14): 1165-1173, 2000.

[9] Zhang Q., Kamata S.I., Pixel colr feature enhancement for road signs detection, *Proceedings of SPIE*, 7546 , 2010.

[10] X.W. Gao, L. Podladchikova, D. Shaposhnikov, Recognition of traffic signs based on their colour and shape features extracted using human vision models, *Journal of Visual Communication and Image Representation,* 17:675-685, 2006.

[11] X.W. Gao, K. Hong, L. Podladchikova, D. Shaposhnikov, P. Passmore, Colour Appearance Based Approaches for Segmentation of Traffic Signs, EURASIP *Journal on Image and Video Processing, vol* 2008, Article ID 386705, 2008.

[12] P. G. Jimenez, S. M. Bascon, A. L. Arroyo, F. L., Ferreras, Traffic sign shape classification and localization based on the normalized FFT of the signature of blobs and 2D homographies, *Signal Processing*, 88(12):2943-2955. 2008.

[13] A. Ruta, Y. Li, X. Liu, Real-time traffic sign recognition from video by class-specific discriminative features, *Pattern Recognition*, 43:416-420, 2010

[14] M. R. Luo, R. W. G. Hunt , The Structure of the CIE 1997 Colour Appearance Model (CIECAM97s), *Color Research and Application*, 23:138-146, 1998.

[15] http://www.cie.co.at/.

[16] Hunt R.W.G. *Measuring Colour*, 2nd ed, Ellis Horwood Limited, 1992.

[17] CIE, The CIE 1997 Interim Colour Appearance Model (Simple Version), CIECAM97s, CIE TC1-34, April, 1998.

[18] I.A., Rybak, V.I., Gusakova, A.V., Golovan, L.N., Podladchikova, N.A., Shevtsova, A Model of Attention-guided Visual Perception and Recognition, *Vision Research*, 38:2387-2400, 1998.

[19] S.J. Sangwine, R.E.N. Horne, *The Colour Image Processing Handbook*, Chapman & Hall, 1998